Limits of Wave Runup and Corresponding Beach-Profile Change from Large-Scale Laboratory Data

Tiffany M. Roberts†, Ping Wang†, and Nicholas C. Kraus‡

†Department of Geology
University of South Florida
4202 East Fowler Avenue
Tampa, FL 33620, U.S.A.
E-mail: tmrobert@cas.usf.edu

‡U.S. Army Engineer Research and
    Development Center
Coastal and Hydraulics Laboratory
3909 Halls Ferry Road
Vicksburg, MS 39180-6199, U.S.A.

ABSTRACT

ROBERTS, T.M.; WANG, P., and KRAUS, N.C., 2010. Limits of wave runup and corresponding beach-profile change from large-scale laboratory data. *Journal of Coastal Research,* 26(1), 184–198. West Palm Beach (Florida), ISSN 0749-0208.

The dataset from the SUPERTANK laboratory experiment was analyzed to examine wave runup and the corresponding upper limit of beach-profile change. Thirty SUPERTANK runs were investigated that included both erosional and accretionary wave conditions with random and monochromatic waves. The upper limit of beach change U_L was found to approximately equal the vertical excursion of total wave runup, R_{tw}. An exception was runs where beach or dune scarps were produced, which substantially limit the uprush of swash motion to produce a much reduced total runup. Based on the SUPERTANK dataset, the vertical extent of wave runup above mean water level on a beach without scarp formation was found to approximately equal the significant breaking wave height, H_{bs}. Therefore, a new and simple relation $R_{tw} = H_{bs}$ is proposed. The linear relationship between total runup and breaking wave height is supported by a conceptual derivation. In addition, the relation is extended to $U_L = R_{tw} = H_{bs}$ to approximate the upper limit of beach change. This formula accurately reproduced the measured upper limit of beach change from the three-dimensional experiments in the Corps' large-scale sediment transport facility. For the studied laboratory cases, predictions of wave runup were not improved by including a slope-dependent surf-similarity parameter. The limit of wave runup was substantially less for monochromatic waves than for random waves, attributed to absence of low-frequency motion.

ADDITIONAL INDEX WORDS: *Beach erosion, nearshore sediment transport, wave breaking, cross-shore sediment transport, physical modeling, surf zone processes.*

INTRODUCTION

Accurate prediction of the upper limit of beach change is necessary for assessing large morphologic changes induced by extreme storms. The upper limit of beach change is controlled by wave breaking and the subsequent wave runup. During storms, wave runup is superimposed on the elevated water level due to storm surge. Wang *et al.* (2006) found the highest elevation of beach erosion induced by Hurricane Ivan in 2004 to be considerably greater than the measured storm-surge level, indicating that wave runup played a significant role in the upper limit of beach erosion. The limit of wave runup is also a key parameter in the application of the storm-impact scale by Sallenger (2000). The Sallenger scale categorizes four levels of morphologic impact by storms through comparison of the highest elevation reached by storm water (combined storm surge and wave runup) and a representative elevation of the barrier island (*e.g.,* the top of the foredune ridge). Quantification of wave runup and its relationship to the upper limit of morphologic change are required for understanding and predicting beach-profile changes.

Wave runup is composed of wave setup and swash runup, defined as a superelevation of the mean water level and fluctuation about that mean, respectively (Guza and Thornton, 1981; Holland *et al.,* 1995; Holman and Sallenger, 1985; Nielsen, 1988; Yamamoto, Tanimoto, and Harshinie, 1994). Several formulas have been developed to predict wave setup and runup. Based on laboratory experiments, Hunt (1959) proposed various formulas estimating wave uprush, *R,* on seawalls and breakwaters, and the "Hunt formula" continues in use:

$$\frac{R}{H} = 1.0 \frac{\tan \beta}{\sqrt{H/L_0}} \tag{1}$$

where $\tan \beta$ = beach slope; H = wave height, typically taken to be the deep-water wave height; and L_0 = deep-water wavelength. Hedges and Mase (2004) modified Hunt's original formula to include the contribution of wave setup.

Bowen, Inman, and Simmons (1968) derived a wave setup slope on a uniformly sloping beach for monochromatic waves as

$$\frac{\partial \bar{\eta}}{\partial x} = -K \frac{\partial h}{\partial x}, \qquad K = (1 + 2.67\gamma^{-2})^{-1} \tag{2}$$

where h = still-water depth, $\bar{\eta}$ = wave setup, x = cross-shore coordinate, and breaker index $\gamma = H/(\bar{\eta} + h)$. Based on both

Report Documentation Page	Form Approved OMB No. 0704-0188

1. REPORT DATE **JAN 2010**	2. REPORT TYPE **N/A**	3. DATES COVERED **-**

4. TITLE AND SUBTITLE **Limits of Wave Runupand Corresponding Beach-Profile Change from Large-Scale Laboratory Data**	5a. CONTRACT NUMBER
	5b. GRANT NUMBER
	5c. PROGRAM ELEMENT NUMBER

6. AUTHOR(S) **Roberts, Tiffany M.; Wang, Ping; and Kraus, Nicholas C.**	5d. PROJECT NUMBER
	5e. TASK NUMBER
	5f. WORK UNIT NUMBER

7. PERFORMING ORGANIZATION NAME(S) AND ADDRESS(ES) **Department of Geology, University of Florida, Tampa, FL; US Army Engineer Research and Developmetn Center, Coastal and Hydraulics Laboratory, Vicksburg, MS**	8. PERFORMING ORGANIZATION REPORT NUMBER

9. SPONSORING/MONITORING AGENCY NAME(S) AND ADDRESS(ES)	10. SPONSOR/MONITOR'S ACRONYM(S)
	11. SPONSOR/MONITOR'S REPORT NUMBER(S)

12. DISTRIBUTION/AVAILABILITY STATEMENT
Approved for public release, distribution unlimited

13. SUPPLEMENTARY NOTES

14. ABSTRACT
Thirty laboratory experiment SUPERTANK runs, including both erosional and accretionary wave conditions with random and monochromatic waves, were analyzed to examine wave runup and the corresponding upper limit of beach-profile change. The upper limit of beach change UL was found to approximately equal the vertical excursion of total wave runup, Rtw. An exception was runs where beach or dune scarps were produced, which substantially limit the uprush of swash motion to produce a much reduced total runup. The vertical extent of wave runup above mean water level on a beach without scarp formation was found to approximately equal the significant breaking wave height, Hbs. Therefore, a new and simple relation Rtw _ Hbs is proposed. This linear relationship is supported by a conceptual derivation. The relation is extended to UL _ Rtw _ Hbs to approximate the upper limit of beach change. This formula accurately reproduced the measured upper limit of beach change from the three-dimensional experiments in the Corps large-scale sediment transport facility. Predictions of wave runup were not improved by including a slope-dependent surf-similarity parameter. The limit of wave runup was substantially less for monochromatic waves than for random waves, attributed to absence of low-frequency motion.

15. SUBJECT TERMS

16. SECURITY CLASSIFICATION OF:			17. LIMITATION OF ABSTRACT	18. NUMBER OF PAGES	19a. NAME OF RESPONSIBLE PERSON
a. REPORT **unclassified**	b. ABSTRACT **unclassified**	c. THIS PAGE **unclassified**	**UU**	**15**	

theory and laboratory measurements, Battjes (1974) found the maximum setup under a monochromatic wave $\bar{\eta}_M$ to occur at the still-water shoreline, $\bar{\eta}_M/H_b = 0.3\gamma$, where H_b = breaking wave height. Taking the commonly used value of 0.78 for γ, the maximum setup yielded from the Battjes formula is about 23% of the breaking wave height.

The development of most formulas predicting the limits for wave runup has involved comparisons to field measurements. Based on measurements made on dissipative beaches, Guza and Thornton (1981) suggested that the setup at the shoreline $\bar{\eta}_{sl}$ is linearly proportional to the significant deep-water wave height H_0:

$$\bar{\eta}_{sl} = 0.17H_0 \tag{3}$$

In a following study, Guza and Thornton (1982) found the significant wave runup R_s (including both wave setup and swash runup) is also linearly proportional to the significant deep-water wave height:

$$R_s = 3.48 + 0.71H_0 \quad \text{(units of centimeters)} \tag{4}$$

Comparing Equations (3) and (4), the entire wave runup is approximately four times the contribution of wave setup, *i.e.,* swash runup constitutes a significant portion, approximately 75%, of the total elevated water level. According to Huntley *et al.* (1993), Equation (4) is the best choice for predicting wave runup on dissipative beaches. Based on field measurements on highly dissipative beaches, Ruesslink, Kleinhans, and van den Beukel (1998) and Ruggiero *et al.* (2001) also found linear relationships, but with slightly different empirical coefficients.

Based on field measurements, Holman (1986) and several similar studies (Holman and Sallenger, 1985; Ruggiero, Holman, and Beach, 2004; Stockdon *et al.,* 2006) argued that more accurate predictions for intermediate beaches can be obtained by including the surf-similarity parameter, ξ, following the Hunt formula (Equation 1):

$$\xi = \frac{\tan\beta}{\sqrt{H_0/L_0}} \tag{5}$$

Holman (1986) found a dependence of the 2% exceedance of runup R_2 on the deep-water significant wave height and the (offshore) surf-similarity parameter:

$$R_2 = (0.83\xi + 0.2)H_0 \tag{6}$$

Stockdon *et al.* (2006) expanded upon the Holman (1986) analysis with additional data covering a wider range of beach slopes and developed the empirical equation:

$$R_2 = 1.1\left\{0.35 \tan\beta_f (H_0 L_0)^{1/2} + \frac{[H_0 L_0(0.563 \tan\beta_f^2 + 0.004)]^{1/2}}{2}\right\} \tag{7}$$

Realizing the variability of beach slope in terms of both definition and measurement, Stockdon *et al.* (2006) defined the foreshore beach slope as the average slope over a region of two times the standard deviation of a continuous water-level record.

With the exception of the original derivation by Bowen, In-man, and Simmons (1968), most predictive formulas for wave runup on a natural beach have been empirically derived based on field measurements over dissipative and intermediate beaches. Field measurements of wave runup were typically conducted with video imagery and/or resistance wire generally 5 to 20 cm above and parallel to the beach face. Holland *et al.* (1995) concluded that these two measurement methods are comparable in producing accurate results.

Almost all the aforementioned field studies focused mainly on the hydrodynamics of wave runup, with little discussion on the corresponding morphologic response, particularly the upper limit of beach-profile change. Thus, in contrast to a considerable number of studies on wave runup, data are scarce that relate the limit of wave runup with the resulting beach change. In other words, the limit of beach change as related to wave runup has not been well documented.

Data from the prototype-scale laboratory experiments, including those conducted at SUPERTANK (Kraus, Smith, and Sollitt, 1992; Kraus and Smith, 1994) and Large-Scale Sediment Transport Facility (LSTF) (Hamilton *et al.,* 2001; Wang, Smith, and Ebersole, 2002), are examined in this paper to study the limit of wave runup and corresponding limit of beach or dune erosion. Specifically, this study examines (1) the levels of total wave runup, including swash runup and wave setup; (2) time-series of beach-profile change under erosional and accretionary waves; (3) the relationship between the waves and beach-profile change; and (4) the accuracy of existing wave runup prediction methods. A new empirical formula predicting the limits of wave runup and that of beach change is proposed based on the prototype-scale laboratory data.

METHODS

SUPERTANK and LSTF Experiments

Data from two movable-bed laboratory studies, SUPERTANK and LSTF (Figure 1), are examined to quantify the upper limits of beach-profile change, wave runup, and their relationship. Both experiments were designed to measure sediment transport and morphology change under varying prototype wave conditions. Dense instrumentation in the laboratory setting allows for well-controlled and accurate measurement of hydrodynamic conditions and morphological change. SUPERTANK was a two-dimensional wave channel with beach change induced primarily by cross-shore processes, whereas the LSTF was a three-dimensional wave basin with both cross-shore and longshore sediment transport inducing beach change.

SUPERTANK was a multi-institutional effort sponsored by the U.S. Army Corps of Engineers and conducted at the O.H. Hinsdale Wave Research Laboratory at Oregon State University from July 29 to September 20, 1991. This facility is the largest wave channel in the United States that can contain a sandy beach through which experiments comparable to the magnitude of naturally occurring waves can be conducted (Kraus, Smith, and Sollitt, 1992). The SUPERTANK experiment measured total-channel hydrodynamics and sediment transport along with the resulting beach-profile change. The wave channel is 104 m long, 3.7 m wide, and 4.6

Figure 1.   The SUPERTANK experiment (top) and LSTF (bottom) during wave runs.

Kraus, 2005). For efficiency, most SUPERTANK cases were initiated with the final profile of the previous run. Approximately 350 profile surveys were made by using an autotracking, infrared Geodimeter targeting prism attached to a survey rod mounted on a carriage pushed by researchers. Three along-channel lines were surveyed. Only the center line was analyzed in this study. Wave-processing procedures are discussed in Kraus and Smith (1994). To separate incident-band wave motion from low-frequency motion, a nonrecursive, low-pass filter was applied. The period cutoff for the filter was set to twice the peak period of the incident waves.

The LSTF is a three-dimensional wave basin located at the U.S. Army Corps of Engineers Coastal and Hydraulic Laboratory in Vicksburg, Mississippi. Operation procedures are discussed in Hamilton *et al.* (2001). The LSTF was designed to study longshore sediment transport (Wang, *et al.,* 2002; Wang, Smith, and Ebersole, 2002). The LSTF is capable of generating wave conditions comparable to the naturally occurring wave heights and periods found along low-energy open coasts and bays. The LSTF has dimensions of 30 m across-shore, 50 m longshore, with walls 1.4 m high (Figure 1 bottom). The beach was designed in a trapezoidal plan shape composed of approximately 150 m³ of very well sorted fine quartz sand with a median grain size of 0.15 mm and a fall speed of 1.8 cm/s. Initial construction of the beach was also based on the equilibrium profile (Equation 8). The beach profile was surveyed using an automated bottom-tracking profiler capable of resolving bed ripples. The beach was typically replenished after 3 to 9 hours of wave activity. Long-crested and unidirectional irregular waves with a relatively broad spectral shape were generated at a 10 degree incident angle in the horizontal section of the basin. The wave height and peak wave period were measured with capacitance wave gauges sampling at 20 Hz, statistical wave properties were calculated by spectral analysis. The experimental procedures in LSTF are described in Wang, Smith, and Ebersole (2002).

Data Analysis

Although the entire SUPERTANK dataset is available, five cases with a total of 30 wave runs were selected from the 20 initial cases. The selection was based on the particular purpose of the wave run, the trend of net sediment transport, and the beach response. Time-series of beach-profile change, cross-shore distribution of wave height, and mean water level were analyzed. Scarp presence was also identified. The upper limits U_L for the nonscarped beach-profile runs were identified based on the upper profile convergence point, above which no beach change occurred. The upper limit identified for the scarped runs was at the elevation of the scarp toe. The other location examined was the lower limit of beach change L_L. The lower limit, or lower profile convergence point, was identified at the depth contour below which no change occurred.

For the 30 SUPERTANK wave runs examined, the water level and zero-moment wave height were analyzed. From the cross-shore wave-height distribution (or wave-energy decay), the breaker point H_b was defined at the location with a sharp decrease in wave height (Wang *et al.,* 2002). The total wave

m deep (the still-water level was typically 1.5 m below the top during SUPERTANK) with a constructed sandy beach extending 76 m offshore (Figure 1 top). The beach was composed of 600 m³ of fine, well-sorted quartz sand with a median size of 0.22 mm and a fall speed of 3.3 cm/s. The wave generator and wave channel were equipped with a sensor to absorb the energy of reflected waves (Kraus and Smith, 1994). The water-level fluctuations were measured with 16 resistance and 10 capacitance gauges. These 26 gauges, spaced no more than 3.7 m apart, provided high resolution of wave propagation, especially in the swash zone.

The beach profile was surveyed following each 20- to 60-minute wave run. The initial profile was constructed based on the equilibrium beach profile developed by Bruun (1954) and Dean (1977) as

$$h(x) = Ax^{2/3} \qquad (8)$$

where h = still-water depth, x = horizontal distance from the shoreline, and A = a shape parameter, which for SUPERTANK corresponded to a median grain size of 0.30 mm. The initial beach was built steeper with a greater A value to ensure adequate water depth in the offshore area (Wang and

Table 1. *Summary of selected wave runs and input wave and beach conditions (notation is explained at the bottom of the table).*

Wave Run ID	H_0 (m)	T_p (s)	L_0 (m)	n	N	H_{bs} (m)	tan β	ξ	$H_{b,h}$ (m)	$H_{b,l}$ (m)	$H_{sl,h}$ (m)	$H_{sl,l}$ (m)
SUPERTANK												
10A_60ER	0.78	3.0	14.0	20	6.4	0.68	0.10	0.42	0.66	0.15	0.13	0.24
10A_130ER	0.78	3.0	14.0	20	6.8	0.68	0.09	0.38	0.67	0.15	0.10	0.23
10A_270ER	0.78	3.0	14.0	20	6.9	0.68	0.10	0.42	0.65	0.16	0.10	0.24
10B_20ER	0.71	3.0	14.0	3.3	6.6	0.65	0.14	0.58	0.63	0.17	0.10	0.23
10B_60ER	0.73	3.0	14.0	3.3	6.8	0.67	0.11	0.44	0.65	0.17	0.11	0.24
10B_130ER	0.72	3.0	14.0	3.3	7.0	0.69	0.09	0.36	0.67	0.18	0.12	0.25
10E_130ER	0.69	4.5	31.6	20	4.9	0.72	0.11	0.69	0.71	0.15	0.15	0.16
10E_200ER	0.69	4.5	31.6	20	5.0	0.74	0.12	0.77	0.72	0.15	0.15	0.18
10E_270ER	0.69	4.5	31.6	20	5.1	0.76	0.09	0.58	0.74	0.15	0.16	0.20
10F_110ER	0.66	4.5	31.6	3.3	5.1	0.75	0.09	0.58	0.72	0.18	0.15	0.26
10F_130ER	0.68	4.5	31.6	3.3	5.1	0.76	0.08	0.48	0.74	0.18	0.13	0.21
10F_170ER	0.69	4.5	31.6	3.3	5.1	0.76	0.08	0.50	0.73	0.20	0.12	0.24
G0_60EM	1.05	3.0	14.0	M	10.0	1.18	0.10	0.43	1.18	0.01	0.11	0.03
G0_140EM	1.04	3.0	14.0	M	10.5	1.04	0.10	0.41	1.04	0.04	0.08	0.10
G0_210EM	1.15	3.0	14.0	M	10.8	1.07	0.09	0.39	1.07	0.04	0.11	0.02
30A_60AR	0.34	8.0	99.9	3.3	1.6	0.41	0.14	2.24	0.40	0.06	0.24	0.08
30A_130AR	0.33	8.0	99.9	3.3	1.6	0.39	0.13	2.09	0.38	0.06	0.24	0.09
30A_200AR	0.34	8.0	99.9	3.3	1.6	0.41	0.13	2.02	0.40	0.06	0.25	0.10
30C_130AR	0.31	9.0	126.4	20	1.4	0.40	0.13	2.36	0.40	0.04	0.18	0.05
30C_200AR	0.31	9.0	126.4	20	1.4	0.39	0.15	2.31	0.38	0.04	0.19	0.06
30C_270AR	0.31	9.0	126.4	20	1.4	0.39	0.15	2.60	0.38	0.04	0.20	0.06
30D_40AR	0.37	9.0	126.4	20	1.4	0.42	0.13	2.00	0.42	0.05	0.17	0.07
I0_80AM	0.60	8.0	99.9	M	2.9	0.76	0.20	2.78	0.76	0.01	0.38	0.03
I0_290AM	0.63	8.0	99.9	M	3.1	0.81	0.17	2.35	0.81	0.01	0.34	0.02
I0_590AM	0.60	8.0	99.9	M	2.7	0.72	0.12	1.64	0.73	0.01	0.25	0.03
60A_40DE	0.69	3.0	14.0	3.3	6.2	0.61	0.12	0.55	0.58	0.14	0.16	0.24
60A_60DE	0.69	3.0	14.0	3.3	6.2	0.61	0.10	0.46	0.60	0.14	0.12	0.24
60B_20DE	0.64	4.5	31.6	3.3	4.4	0.66	0.11	0.74	0.63	0.15	0.18	0.24
60B_40DE	0.63	4.5	31.6	3.3	4.4	0.66	0.11	0.76	0.62	0.16	0.18	0.25
60B_60DE	0.65	4.5	31.6	3.3	4.4	0.66	0.12	0.79	0.63	0.17	0.18	0.30
LSTF												
Spilling	0.27	1.5	3.5	3.3	10.0	0.26	0.11	0.41	N/C	N/C	N/C	N/C
Plunging	0.24	3.0	14.0	3.3	4.4	0.27	0.13	0.96	N/C	N/C	N/C	N/C

H_0 = offshore wave height; T_p = peak wave period; L_0 = offshore wavelength; n = spectral peakedness; N = Dean number; H_{bs} = significant breaking wave height; tan β = beach slope defined as the slope of the section approximately 1 m landward and 1 m seaward of the shoreline; ξ = surf-similarity parameter; $H_{b,h}$ = incident-band wave height at the breaker line; $H_{b,l}$ = low-frequency band wave height at the breaker line; $H_{sl,h}$ = incident-band wave height at the shoreline; $H_{sl,l}$ = low-frequency band wave height at the shoreline; M = monochromatic wave; N/C = Not calculated.

runup R_{tw} was defined by the location and beach elevation of the swash gauge that contained a value larger than zero wave height, *i.e.,* water reached that particular gauge. The above procedure did not involve any statistical analysis but rather was determined by the measurements available from SU-PERTANK. Hence, there may be some differences between the R_{tw} determined in this study and the 2% exceedance of runup ($R_{2\%}$) as appears in some predictive equations, obtained from video (*e.g.,* Holland *et al.,* 1995) and horizontally elevated wires (*e.g.,* Guza and Thornton, 1982).

Two LSTF experiments, one conducted under random spilling breaker waves and one under random plunging breaker waves, were examined in this study. The LSTF data were examined for the upper limit of beach change. The beach profiles analyzed here were surveyed through the middle of the basin. The maximum runup was not directly measured due to the lack of swash gauges. The main objective of the LSTF analysis was to apply the SUPERTANK results to a three-dimensional beach.

RESULTS

Overall, 30 SUPERTANK wave runs and two LSTF wave cases were analyzed (Table 1). The two LSTF cases, under a

spilling and a plunging breaker, examined the effect of the breaker types on sediment transport and the resulting beach-profile change. The 30 SUPERTANK wave runs are composed of 12 erosional random wave runs, three erosional monochromatic wave runs, seven accretionary random wave runs, three accretionary monochromatic wave runs, and five dune erosion random wave runs. In Table 1, the first two numbers in the wave run ID "10A_60ER" indicate the major data collection case, the letter "A" indicates a particular wave condition, and the numerals indicate the duration of wave action in minutes. The notation used in Table 1 and in all equations is listed in Appendix I. The erosional and accretionary cases were designed based on the Dean number *N,*

$$N = \frac{H_{bs}}{wT} \qquad (9)$$

where H_{bs} = significant breaking wave height; w = fall speed of the sediment, and T = wave period (Kraus, Smith, and Sollitt, 1992).

Beach-Profile Change

Analysis of the time-series of beach-profile change for the SUPERTANK experiment can be found in Roberts, Wang,
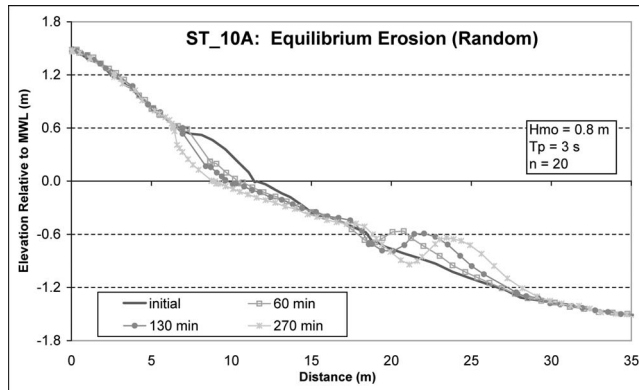
Figure 2.   The first SUPERTANK wave run, ST_10A erosional case. Substantial shoreline erosion occurred on the initial monotonic profile with the development of an offshore bar. The horizontal axis "distance" refers to the SUPERTANK coordinate system and is not directly related to morphological features.

and Kraus (2007). The first SUPERTANK wave run, ST_10A, was conducted with a monotonic initial profile (Equation 8). Figure 2 illustrates four time-series beach profiles surveyed at the beginning, 60, 130, and 270 minutes. The design wave conditions are included as an inset in the figures, where H_{mo} is the zero-moment wave height, T_p is the peak spectral wave period, and n is spectral peakedness. Significant beach-profile change occurred with substantial shoreline recession, along with the development of an offshore bar. Initially, the foreshore exhibited a convex shape while the end profile was concave. The upper limit of beach-profile change was measured at 0.66 m above mean water level (MWL) for all three time segments. An apparent point of profile convergence was measured at the 1.35-m depth contour, beyond which profile elevation change cannot be clearly identified.

The subsequent wave runs were conducted over the final profile of the previous wave run, i.e., over a barred beach. The beach-profile changes are detectable but much more subtle than the initial run (Figure 2), especially for the accretionary wave runs with lower wave heights. Figure 3 shows an example of an accretionary wave run, ST_30A. The upper limit was determined to be at 0.31 m above MWL (Figure 3 bottom). One of the surveys (60 min) exhibited some changes above that convergence level; however, these changes may be attributable to survey error. The offshore-profile convergence point was determined at a depth contour of around 1 m.

A scarp developed in some of the erosional wave runs (Figure 4). The scarp was induced by wave erosion of the base of the dune or the dry beach, subsequently causing the overlying sediment to become unstable and collapse. The resulting beach slope directly seaward of the scarp tends to be steeper than on a nonscarped beach. The upper limit of beach change is apparently at the top of the scarp, controlled by the elevation of the beach berm or dune, and does not necessarily represent the vertical extent of wave action. The upper limit of beach change in this study was selected at the base of the near-vertical scarp, measured at 0.31 m above MWL during
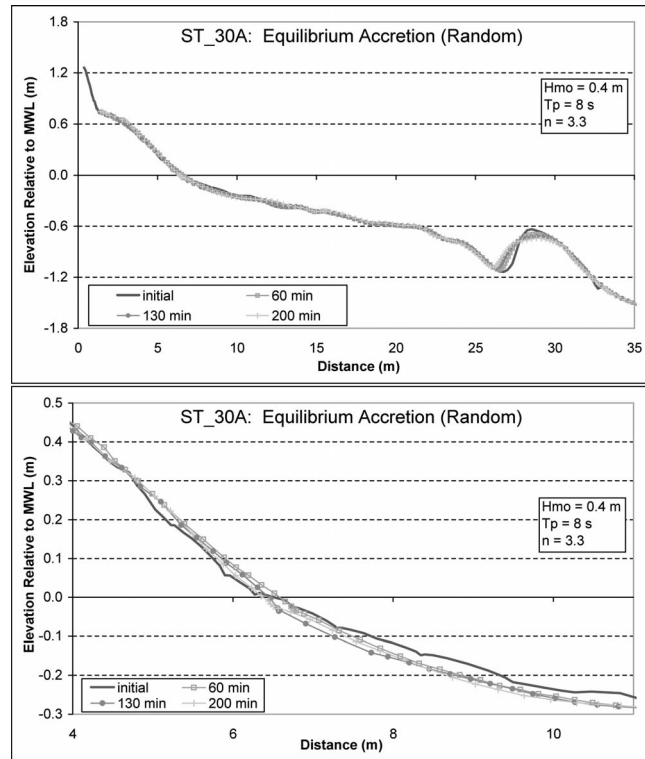

Figure 3.   The SUPERTANK ST_30A accretionary wave run. There was subtle beach-face accretion, with an onshore migration of the offshore bar (top). The accretion near the shoreline is identified if viewed at local scale (bottom).

ST_60A (Figure 4). Therefore, for the scarped case, the upper limit was controlled by both wave action and gravity-driven dune collapse. Little beach-profile change was observed offshore.

SUPERTANK experiments also included several runs with monochromatic waves. Beach-profile change under mono-
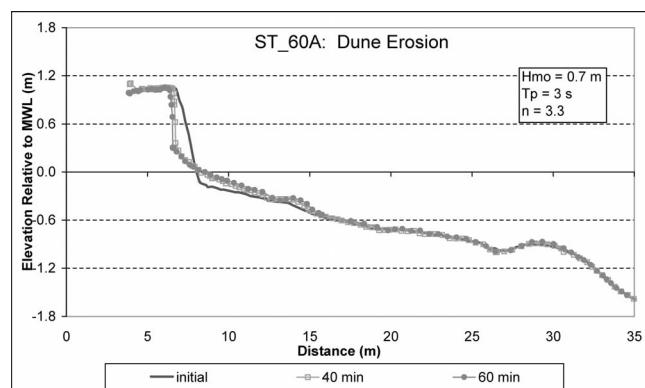

Figure 4.   The SUPERTANK ST_60A dune erosion wave run. A nearly vertical scarp developed after 40 min of wave action, with the upper limit of beach change identified at the toe of the dune scarp.
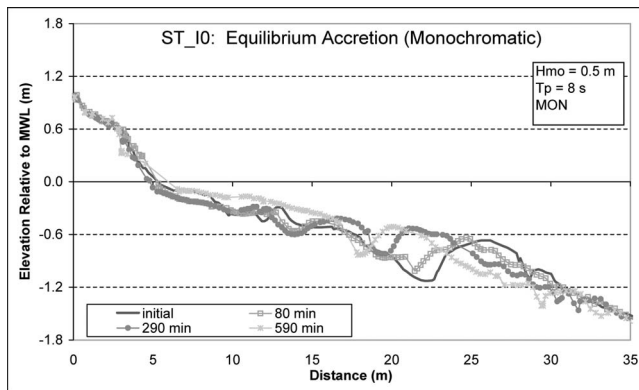
Figure 5. The SUPERTANK ST_I0 accretionary monochromatic wave run. The resulting beach profile under monochromatic waves is erratic and undulating.

chromatic wave action was substantially different from those under the more realistic random waves (Figure 5). The monochromatic waves tended to create erratic and undulating profiles. For ST_I0, the upper limit of beach-profile change was estimated at around 0.50 m and varied slightly during the
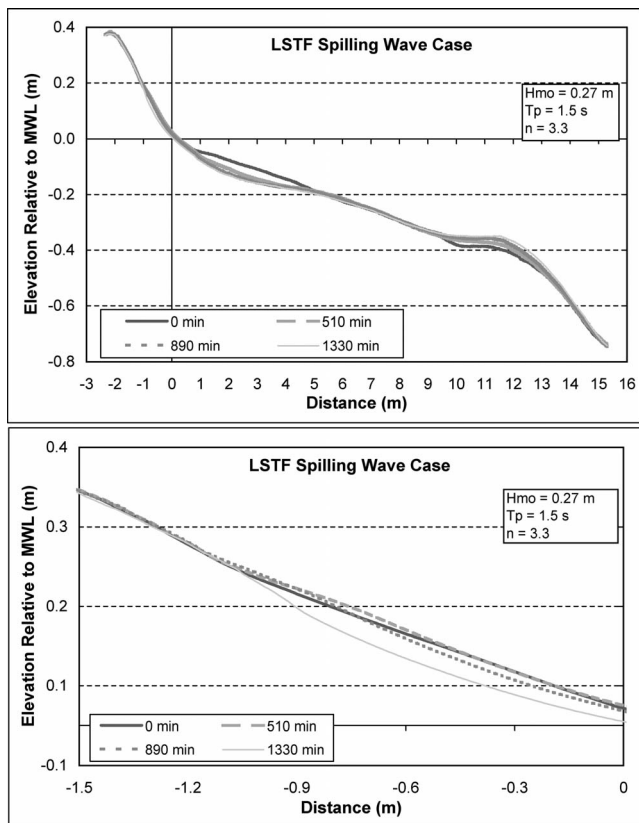

Figure 6. The LSTF spilling wave case. Erosion occurred in the foreshore and inner surf zone. The eroded sediment was deposited on an offshore bar.
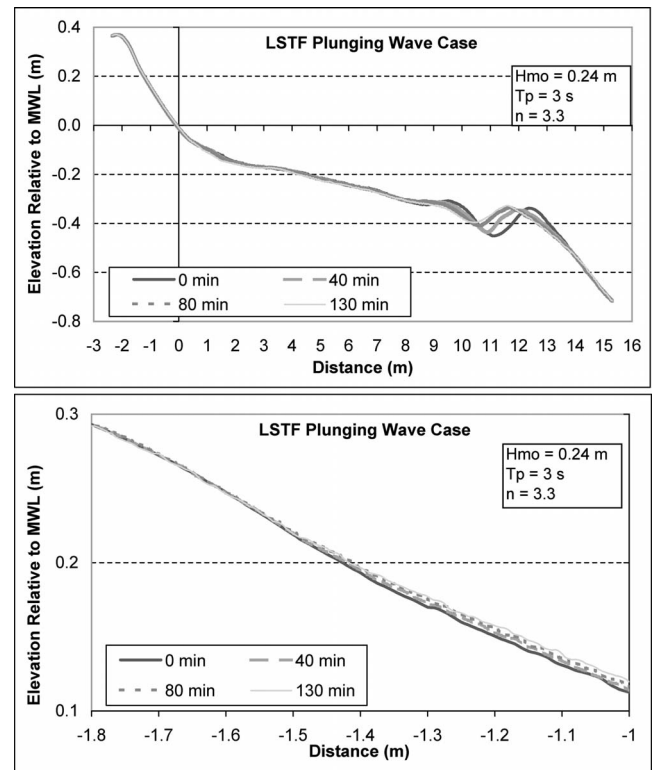

Figure 7. The LSTF plunging wave case. Slight foreshore accretion and landward migration of the offshore bar occurred during the wave run.

different wave runs. The erratic profile evolution did not seem to approach a stable equilibrium shape, and it did not have an apparent profile convergence point. In addition, the profile shape developed under monochromatic waves does not represent profiles typically measured in the field (Wang and Davis, 1998). This implies that morphological change measured in movable-bed laboratory experiments under monochromatic waves may not be applicable to a natural setting.

Similar analyses were also conducted for the data from the LSTF. The waves generated in the LSTF had smaller heights and shorter periods as compared with the SUPERTANK waves. Two cases with distinctively different breaker types, one spilling and one plunging, were examined.

The spilling wave case was initiated with the Dean equilibrium beach profile (Equation 8). Because of the smaller wave heights, beach-profile change occurred at a slower rate. Similar to the first SUPERTANK wave run, ST_10A, a subtle bar formed over the initial monotonic beach profile (Figure 6 top). For the spilling wave case, the upper limit of beach change was 0.23 m above MWL, as identified from the smaller scale plot (Figure 6 bottom). The profile converges on the seaward slope of the offshore bar. For the LSTF plunging wave case, shoreline advance occurred with each wave run along with sustained onshore migration of the bar (Figure 7). The accumulation at the shoreline was subtle but can be identified if viewed locally (Figure 7 bottom). The upper limit of beach-profile change was located at 0.26 m above MWL,

Table 2. *Summary of beach change and breaking wave height.*

Wave Run ID	H_{bs} (m)	U_L (m)	L_L (m)	Scarp
SUPERTANK				
10A_60ER	0.68	0.66	1.29	No
10A_130ER	0.68	0.66	1.29	No
10A_270ER	0.68	0.66	1.29	No
10B_20ER	0.65	0.67	1.35	No
10B_60ER	0.67	0.67	1.35	No
10B_130ER	0.69	0.67	1.35	No
10E_130ER	0.72	0.74	1.52	No
10E_200ER	0.74	0.84	1.52	No
10E_270ER	0.76	0.84	1.52	No
10F_110ER	0.75	0.43	1.52	Yes
10F_130ER	0.76	0.42	1.52	Yes
10F_170ER	0.76	0.48	1.52	Yes
G0_60EM	1.18	0.38	1.61	No
G0_140EM	1.04	0.25	1.61	Yes
G0_210EM	1.07	0.27	1.61	Yes
30A_60AR	0.41	0.31	1.36	No
30A_130AR	0.39	0.31	1.36	No
30A_200AR	0.41	0.31	1.36	No
30C_130AR	0.40	0.39	1.01	No
30C_200AR	0.39	0.42	1.01	No
30C_270AR	0.39	0.42	1.01	No
30D_40AR	0.42	0.43	0.65	No
I0_80AM	0.76	0.46	1.82	No
I0_290AM	0.81	0.53	1.82	No
I0_590AM	0.72	0.53	1.82	Yes
60A_40DE	0.61	0.28	1.16	Yes
60A_60DE	0.61	0.28	1.16	Yes
60B_20DE	0.66	0.38	0.99	Yes
60B_40DE	0.66	0.38	0.99	Yes
60B_60DE	0.66	0.38	0.99	Yes
LSTF				
Spilling	0.26	0.23	0.62	No
Plunging	0.27	0.26	0.50	No

U_L, L_L = upper and lower limit of beach change, respectively.

Figure 8. Cross-shore wave-height distribution measured during SU-PERTANK ST_10A.

with the lower limit identified at the profile convergence point midway on the seaward slope of the bar. Overall, the trends observed in the three-dimensional LSTF experiment are comparable to those in the two-dimensional SUPER-TANK experiment.

Table 2 summarizes the upper and lower limits of change during each wave run, including the breaking wave height. In summary, for the 30 SUPERTANK wave runs and two LSTF wave cases, the incident breaking wave height ranged from 0.26 to 1.18 m (Table 2). The measured upper limit of profile change, including the scarped dune cases, ranged from 0.23 to 0.70 m. The lower limit of beach change ranged from 0.50 to 1.61 m below MWL. Relationships between the profile change and wave conditions are discussed in the following sections.

Cross-Shore Distribution of Wave Height

Wave-height decay is representative of the energy dissipation as a wave propagates onshore. Wave decay patterns were measured by the closely spaced gauges for both the SU-PERTANK and the LSTF experiments. Figure 8 shows time-series wave decay patterns measured at the first SUPER-TANK wave run, ST_10A. As discussed above, considerable beach-profile change, for example the formation of an off-
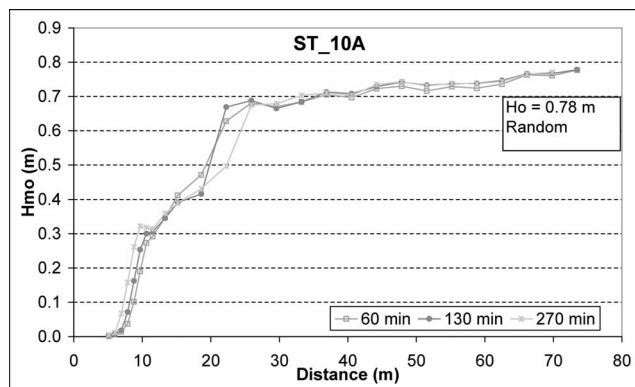
shore bar, was produced during this wave run (Figure 2). The substantial morphology change also influenced the pattern of wave decay. The point of steep wave decay migrated slightly as the beach morphology changed from the initial monotonic profile to a barred-beach profile. This point was defined as the location and height at which the wave breaks (Wang *et al.,* 2002). For ST_10A, the significant breaking wave height was 0.68 m. The rate of wave-height decay tended to be smaller in the middle surf zone (10 to 20 m) as compared with the breaker zone (20 to 25 m) and the inner surf zone (landward of 10 m). The offshore wave height remained largely constant until reaching the breaker line.

The wave decay pattern for the longer period accretionary wave run, ST_30A (Figure 9), was considerably different than the steep erosive waves. The significant breaking wave height was 0.36 m. The time-series wave pattern remained constant for each wave run, apparently not influenced by the subtle morphology change (Figure 3). The bar was formed during the previous wave runs with greater wave heights. Therefore, instead of breaking over the bar, shoaling or increase in height of the long-period wave was measured (at
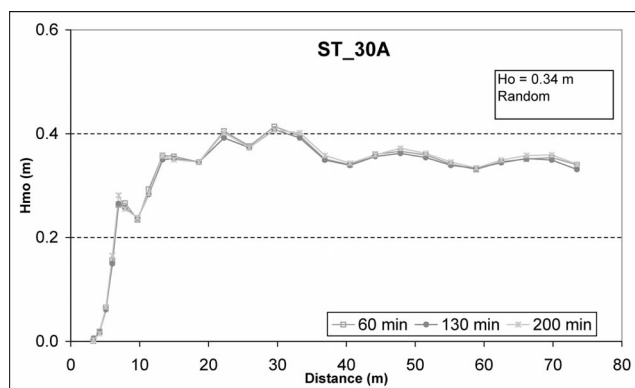

Figure 9. Cross-shore wave-height distribution measured during SU-PERTANK ST_30A.
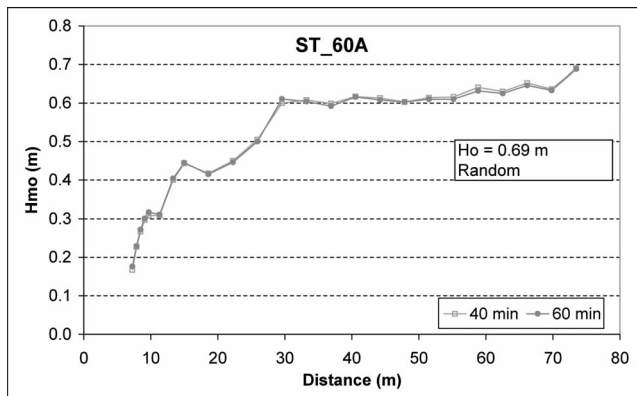
Figure 10. Cross-shore wave-height distribution measured during SUPERTANK ST_60A.

Figure 12. Cross-shore wave-height distribution for the LSTF spilling and plunging wave cases.

around 30 m). The main breaker line was identified at around 15 m, where a sharp drop in wave height was observed.

For the dune erosion run, ST_60A, the wave height remained largely constant offshore (Figure 10). Significant wave-height decay was measured over the offshore bar at approximately 30 m, with a breaker height of 0.61 m. A noticeable increase in wave height was measured at around 15 m offshore, likely a result of reflected waves off the scarp, followed by a sharp decrease in height in the inner surf zone.

The cross-shore distribution of wave height for the monochromatic wave run ST_I0 was erratic with both temporal and spatial irregularity (Figure 11). The erratic wave-height distribution corresponds to the irregular beach-profile change observed during this wave run (Figure 5). The breaking wave height varied considerably, from 0.72 to 0.81 m, likely caused by reflection of the monochromatic waves from the beach face. The wave-height variation in the offshore region, seaward of the breaker line around 30 m, was likely related to oscillations in the wave tank.

The LSTF experiments were designed to examine the effects of different breaker types on sediment transport and
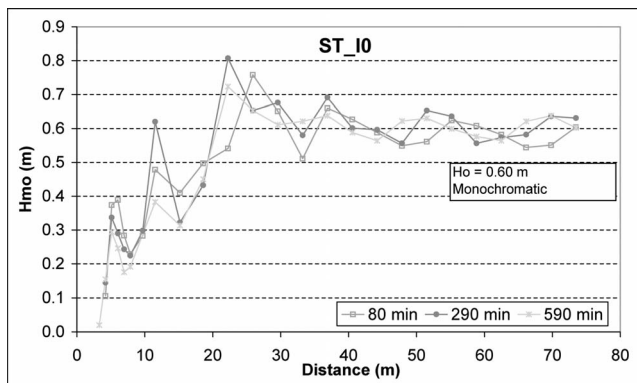
morphology change. Offshore wave heights of 0.27 m were generated for both cases (Figure 12), which had different wave periods. However, the cross-shore distribution of wave heights was considerably different. The wave-height decay at the breaker line was much greater for the plunging case than for the spilling case, as expected. The breaking wave height was 0.26 m and 0.27 m for the spilling and plunging wave runs, respectively.

Wave Runup

The extent and elevation of wave runup for the SUPERTANK experiments were measured directly by the closely spaced swash gauges (Kraus and Smith, 1994). Figure 13 shows the cross-shore distribution of time-averaged water level and wave runup for the erosive wave run, ST_10A. The swash zone water level was measured by the discrete swash gauges, as discussed above, and does not represent time-averaged water level. Elevated water levels were measured in the surf zone. As expected, the mean water level in the off-
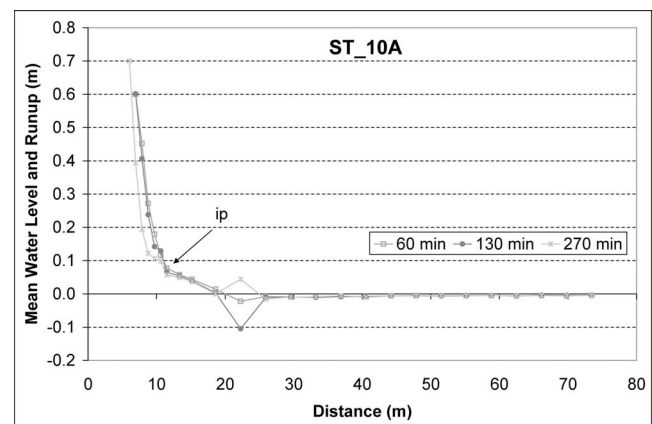

Figure 11. Cross-shore wave-height distribution measured during SUPERTANK ST_I0.

Figure 13. Wave runup measured during SUPERTANK ST_10A. The arrow with notation "ip" refers to the inflection point between the wave setup and runup.
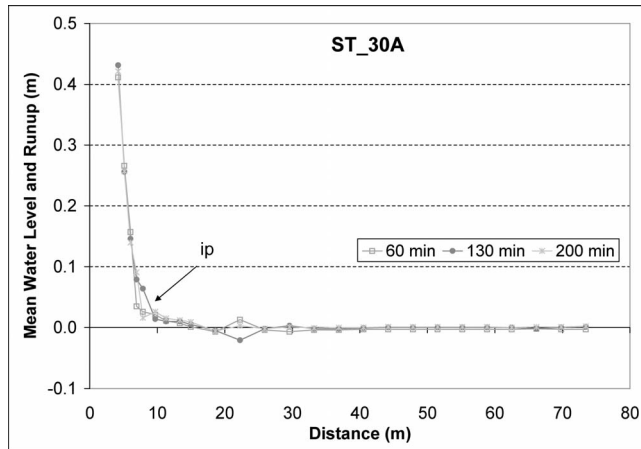
Figure 14. Wave runup measured during SUPERTANK ST_30A. The arrow with notation "ip" refers to the inflection point between the wave setup and runup.

Figure 15. Wave runup measured during SUPERTANK ST_60A. The arrow with notation "ip" refers to the inflection point between the wave setup and runup.

shore area remained around zero. It is necessary to separate the elevation caused by wave setup and swash runup. An inflection point (labeled with an arrow and "ip") can be identified from the cross-shore distribution curve of the mean water level (Figure 13). The inflection point also tends to occur around the still-water shoreline and is regarded here as the distinction between wave setup and swash runup. For this run, the setup measured at the still-water shoreline was 0.1 m, which is about 17% of the total wave runup of 0.6 m.

For the accretionary wave run, ST_30A, the inflection point in the mean water level also occurs around the still-water shoreline (Figure 14). The average setup at the shoreline was approximately 0.07 m, also about 17% of the total wave runup of 0.4 m. Total wave runup was significantly limited by the vertical scarp as shown in the dune erosion run of ST_60A (Figure 15). A broad setdown was measured just seaward of the main breaker line. The inflection point of the cross-shore distribution of the mean water level occurred between 10 and 11 m, before reaching the still-water shoreline at 8 m. The setup measured at the inflection point at 11 m was approximately 0.03 m. The wave setup contributed 18% of the total wave runup of 0.17 m, similar to the above two cases.

The cross-shore distribution of time-averaged mean water level and wave runup for ST_I0 (monochromatic waves) was erratic (Figure 16). As opposed to the irregular wave cases, a zero mean water level was not measured at a considerable number of offshore wave gauges. In addition, significant variances among different wave runs were also measured. The total wave runup varied from 0.16 to 0.35 m, with an average of 0.26 m. The inflection point in the mean water level distribution occurs around the still-water shoreline at 5 m. The maximum setup at the still-water shoreline was 0.08 m, which is 31% of the total wave runup. The smaller contribution of the swash runup to the total wave runup can be attributed to the lack of low-frequency motion in the monochromatic waves.
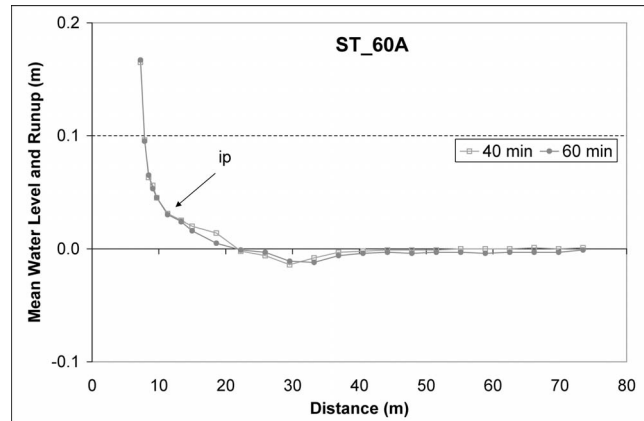
DISCUSSION

Relationship between Wave Runup, Incident Wave Conditions, and Limit of Beach-Profile Change

The measured breaking wave height, upper limit of beach-profile change, and total wave runup from the SUPERTANK experiments are compared in Figure 17. The 30 runs examined are divided into three categories describing nonscarped random wave runs, scarped random wave runs, and monochromatic wave runs. For the 16 nonscarped random wave runs, except the three runs (10B_20ER, 10E_270ER, and 30D_40AR), the elevations of wave runup and upper limit of beach change roughly equal the significant breaking wave height. All three outliers had relatively lower measured swash runup. The discrepancy may be caused by the performance of the capacitance gauge. The partially buried capacitance gauges in the swash zone required the sand to be fully
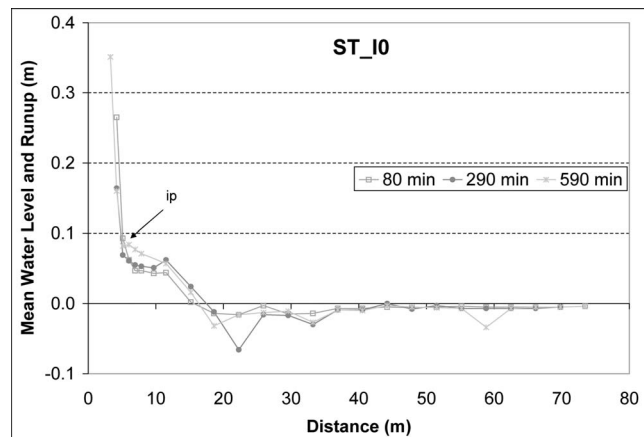

Figure 16. Wave runup measured during SUPERTANK ST_I0. The arrow with notation "ip" refers to the inflection point between the wave setup and runup.
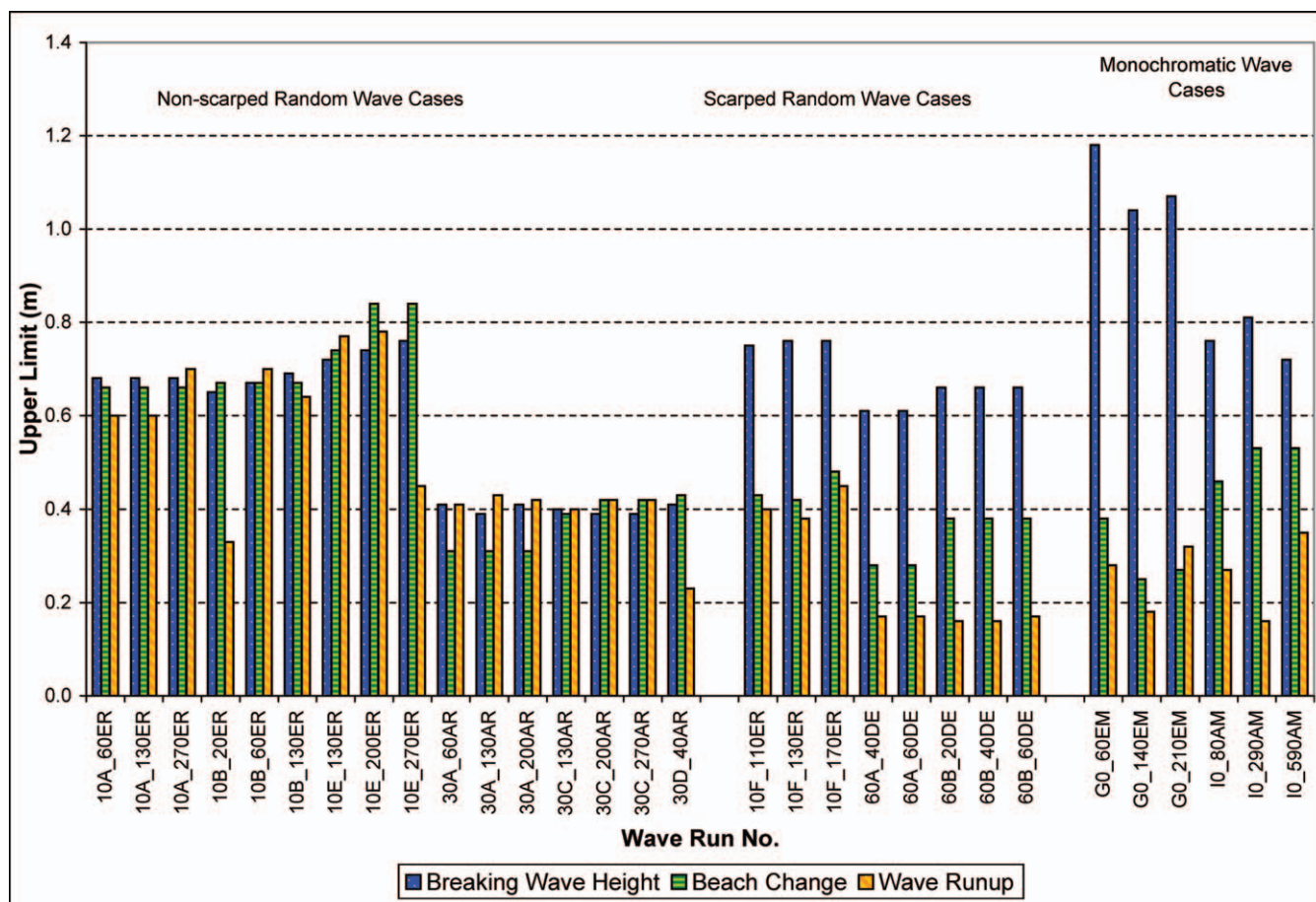
Figure 17. Relationship between breaking wave height, upper limit of beach-profile change, and wave runup for the 30 SUPERTANK cases examined.

saturated (Kraus and Smith, 1994). Both 10B_20ER and 30D_40AR are initial short-duration runs, during which the sand may not have been fully saturated. However, this does not explain the discrepancy for 10E_270ER, with cause unknown.

For the scarped random wave runs, the breaking wave height was much greater than the elevation of wave runup, which was limited by the vertical scarp. Because the upper limit of beach change was identified at the toe of the scarp, a relationship among the breaker height, wave runup, and beach-profile change is not expected for the scarped random wave runs. The much lower wave runup by monochromatic waves as compared with the breaker height was likely caused by the lack of low-frequency motion. No relationship could be found among the three parameters for monochromatic waves.

Based on the above observations from the SUPERTANK data with breaking wave heights ranging from 0.4 to 1.2 m (Figure 17), a simple relationship between the measured wave runup height on a nonscarped beach and the breaker height is found:

$$R_{tw} = 1.0 H_{bs} \qquad (10)$$

The average ratio of R_{tw} over H_{bs} for the 16 nonscarped wave runs was 0.93, with a standard error on the mean of 0.05. Excluding the three questionable measurements, 10B_20ER, 10E_270ER, and 30D_40AR, the average R_{tw}/H_{bs} was 1.01, with a standard error of 0.02. To be conservative because of limited data coverage, a value of 1.0 was assigned in Equation (10). Caution should be exercised in applying Equation (10) to higher waves than the range examined here.

Comparisons of the measured wave runup with the various existing empirical formulas (Equations 4, 6, and 7) and Equation (10) are summarized in Figure 18 and Table 3. It is recognized that Equation (4) predicts significant runup height, whereas Equations (6) and (7) predict 2% exceedance of runup. The measured runup R_{tw} from SUPERTANK represents a maximum value of total wave runup (Equation 10). As shown in Figure 18, previous formulas did not reproduce the measured wave runup at SUPERTANK. For the 16 nonscarped wave runs, 81% of the predictions from Equation (10) fall within 15% of the measured wave runup. In contrast, for Equations (4), (6), and (7), only 25%, 6%, and 13% of the predictions, respectively, fall within 15% of the measured values.
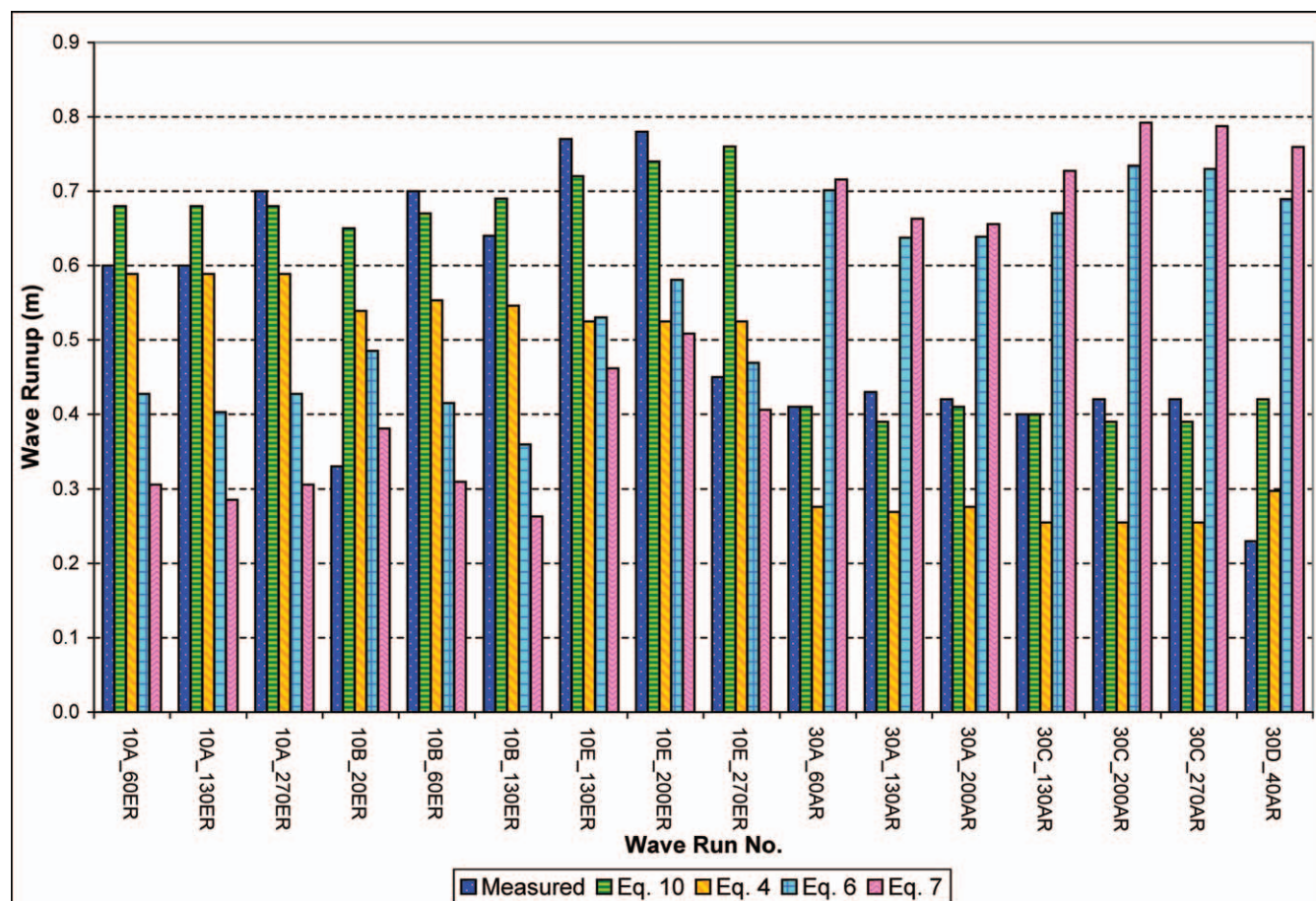
Figure 18. Comparison of measured and predicted wave runup.

Equations (6) and (7) underpredicted the measured wave runup significantly for the erosional cases, but overpredicted runup for the accretionary wave cases. The discrepancy is caused by the substantially greater value of ξ for the gentle long-period accretionary waves than for the steep short-period erosional waves (Table 1). Agreement between measured and predicted values was reduced by including the surf-similarity parameter, ξ. The simpler Equation (4) developed by Guza and Thornton (1982) based only on the offshore wave height more accurately reproduced the measured values of wave runup than Equations (6) and (7).

Equation (10) was applied to the three-dimensional LSTF experiments with lower wave heights than in SUPERTANK. Although wave runup was not directly measured in the LSTF experiments, it is assumed here that the total runup is equal to the upper limit of beach-profile change, a reasonable assumption as verified by the SUPERTANK data. For the spilling wave case, taking the upper limit of beach change at 0.23 m as the value for total wave runup, the breaking wave height of 0.26 m resulted in an overprediction of 13%. For the plunging wave case, the upper limit of beach change was 0.26 m, which is almost equal to the 0.27-m breaking wave height.

Table 3. *Summary of measured and predicted wave runup.*

Wave Run ID	H_{bs} (m)	R_{tw} (m)	Equation (4) (m)	Equation (6) (m)	Equation (7) (m)	Equation (10) (m)
110A_60ER	0.68	0.60	**0.59**	0.43	0.31	**0.68**
110A_130ER	0.68	0.60	**0.59**	0.40	0.29	**0.68**
10A_270ER	0.68	0.70	0.59	0.43	0.31	**0.68**
10B_20ER	0.65	0.33	0.54	0.49	**0.38**	0.65
10B_60ER	0.67	0.70	0.55	0.42	0.31	**0.67**
10B_130ER	0.69	0.64	**0.55**	0.36	0.26	**0.69**
10E_130ER	0.72	0.77	0.52	0.53	0.46	**0.72**
10E_200ER	0.74	0.78	0.52	0.58	0.51	**0.74**
10E_270ER	0.76	0.45	**0.52**	**0.47**	**0.41**	0.76
30A_60AR	0.41	0.41	0.28	0.70	0.72	**0.41**
30A_130AR	0.39	0.43	0.27	0.64	0.66	**0.39**
30A_200AR	0.41	**0.42**	0.28	0.64	0.66	**0.41**
30C_130AR	0.40	0.40	0.25	0.67	0.73	**0.40**
30C_200AR	0.39	0.42	0.25	0.73	0.79	**0.39**
30C_270AR	0.39	0.42	0.25	0.73	0.79	**0.39**
30D_40AR	0.42	0.23	0.30	0.69	0.76	0.42

Bold type indicates predicted values that fall within 15% of the measured runup. R_{tw} = total measured wave runup.
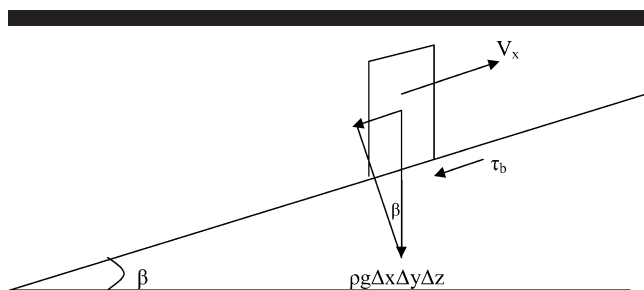
Figure 19. Forces acting on a water element in the swash zone.

Therefore, the LSTF data, with a finer grain size (0.15 mm) than SUPERTANK (0.22 mm), support the new predictive equation (Equation 10).

The dependence of wave runup on beach slope has been questioned by various studies. Douglass (1992) reanalyzed the Holman (1986) dataset underlying development of Equation (6) and stated that runup and beach-face slope are not well correlated. Douglass argued that beach slope is a dependent variable that is free to respond to the incident waves and should not be included in runup prediction. Sunamura (1984) and Kriebel, Kraus, and Larson (1991) found dependencies of beach slope on wave height and period, the latter reference giving a predictive formula expressed in terms of the Dean number (Equation 9). Nielsen and Hanslow (1991) found a relationship between the surf-similarity parameter and runup on steep beaches. However, for gentle beaches with slopes less than 0.1, they suggested that the surf-similarity parameter was not related to runup. A subsequent study by Hanslow and Nielson (1993) conducted on dissipative beaches of Australia found that maximum setup did not depend on beach slope.

In practice, beach-face slope is a difficult parameter to define and determine. Except for Stockdon *et al.* (2006), a clear definition of beach slope is not given in most studies. Stockdon *et al.* defined the foreshore beach slope as the average slope over a region of two times the standard deviation of a continuous water-level record. In predictive modeling of morphology change, relations between runup and foreshore slope would be interdependent. In the present study, the slope was defined over the portion of the beach extending roughly 1 m landward and seaward from the shoreline. Substantially different beach slopes can be obtained by imposing different definitions. Inclusion of the beach slope in predictive relations for wave runup thus adds ambiguity in applying such formulations.

Determining offshore wave height may also introduce uncertainty. In most field studies, the offshore wave height is taken to be the measurement at a wave gauge in the study area. Similarly, in this study it is taken as the wave height measured at the farthest offshore gauge. The definition of an offshore wave height varies between studies, in which it is often taken at whatever depth the instrument is deployed (Guza and Thornton, 1981, 1982; Holman, 1986). In addition, under storm conditions, estimation of the offshore wave height may not be straightforward (Wang *et al.*, 2006).

A Conceptual Derivation of the Proposed Wave Runup Model

Swash uprush on a sloping beach is often approximated using a ballistics approach of bore propagation (Baldock and Holmes, 1999; Coco, O'Hare, and Huntley, 1999; Larson, Kubota, and Erikson, 2004; Mase, 1988; Suhayda, 1974). Most derivations are based on the bore runup model of Shen and Meyer (1963) and the radiation stress formulation of Longuet-Higgens and Stewart (1962). In the following derivation, a similar approach is adopted to examine the physics foundation of Equation (10).

Assuming a normally incident wave and neglecting longshore variations, the forces acting on a water element in the swash zone in the cross-shore direction, x (Figure 19), can be balanced as

$$-\rho g \, \Delta x \, \Delta y \, \Delta z \, \sin \beta - \frac{f}{8} \rho \, \Delta x \, \Delta y \, V_x^2 = \rho \, \Delta x \, \Delta y \, \Delta z \frac{\partial V_x}{\partial t} \quad (11)$$

ρ = density of water; g = acceleration due to gravity; $\Delta x, \Delta y,$ and Δz = length, width, and height of the water element, respectively; $\sin \beta$ = beach slope; f = friction coefficient; and V_x = velocity. Equation (11) can be reduced to

$$\frac{\partial V_x}{\partial t} = -g \, \sin \beta - \frac{f}{8 \Delta z} V_x^2 \quad (12)$$

Assuming the friction force is negligible, an assumption supported by experiments discussed in Komar (1998), Equation (12) is further reduced to

$$\frac{\partial V_x}{\partial t} = -g \, \sin \beta \quad (13)$$

Influences of friction and infiltration on swash motion are discussed in Puleo and Holland (2001). Integrating Equation (13) with respect to time yields

$$V_x = V_0 - gt \, \sin \beta \quad (14)$$

where V_0 = initial velocity. Integrating Equation (14) again with respect to time gives the swash excursion, $x,$ as a function of time, t:

$$x(t) = V_0 t - \frac{gt^2}{2} \sin \beta \quad (15)$$

From Equation (14), the maximum uprush occurs at a time, t_{max}, when the velocity becomes zero:

$$t_{max} = \frac{V_0}{g \, \sin \beta} \quad (16)$$

with a corresponding value of maximum swash excursion of

$$x(t_{max}) = \frac{V_0^2}{2g \, \sin \beta} \quad (17)$$

Assuming a small and planar foreshore slope, then $\tan \beta \approx \sin \beta$, and the elevation of the maximum swash uprush, R_{sr_max}, becomes

$$R_{sr\_max} = x(t_{max}) \tan \beta = \frac{V_0^2}{2g \, \sin \beta} \tan \beta \approx \frac{V_0^2}{2g} \quad (18)$$

Equation (18) suggests that the maximum elevation of swash

runup is not a function of beach slope if bottom friction forcing is neglected.

The initial velocity V_0 can be approximated by the velocity of the wave, C. In shallow water, the wave velocity is limited by the local water depth, h_l,

$$V_0 \approx C = \sqrt{gh_l} \qquad (19)$$

Assuming a linear relationship between local breaking or breaking wave height, H_{bl}, and the water depth, h_l

$$H_{bl} = \gamma h_l \qquad (20)$$

where γ = the breaker index. Equation (19) then becomes

$$V_0^2 \approx C^2 = g\frac{H_{bl}}{\gamma} \qquad (21)$$

Substituting Equation (21) into Equation (18)

$$R_{sr\_max} = \frac{V_0^2}{2g} = \frac{gH_{bl}}{2g\gamma} = \frac{H_{bl}}{2\gamma} \qquad (22)$$

Because of wave height to depth scaling in the surf zone, it is reasonable to assume that the initial velocity V_0 can be taken at the main breaker line. With significant breaker height H_{bs} Equation (22) then becomes

$$R_{sr\_max} = \frac{H_{bs}}{2\gamma} = \alpha H_{bs} \qquad (23)$$

where $\alpha = \frac{1}{2\gamma}$. Equation (23) indicates a linear relationship between breaking wave height and the maximum swash runup, supporting the findings deduced from the SUPERTANK experiment.

Kaminsky and Kraus (1994) examined a large dataset on breaking wave criteria that included both laboratory and field measurements. They found the majority of γ values range from 0.6 to 0.8, which yields α values from 0.63 to 0.83. Based on previous discussion (Figures 13 through 16), swash runup constitutes approximately 83% of the total wave runup. Adding the 17% contribution from the wave setup, the total wave runup R_{tw} is roughly equal to the breaking wave height, further supporting the predictive equation developed from the SUPERTANK dataset. Thus, the empirical model of total wave runup developed based on the SUPERTANK data is supported by an accepted physical picture. In addition, little ambiguity exists in the straightforward parameterization as given in Equation (10).

CONCLUSIONS

The SUPERTANK data set indicates that the vertical extent of wave runup above mean water level on a nonscarped beach is approximately equal to the significant breaking wave height. A simple formula for predicting the total wave runup, $R_{tw} = 1.0H_{bs}$, was developed by comparison with measurements and justified by a derivation based on ballistic theory of swash motion. This formula does not include beach slope, which is difficult to measure and is itself dependent on wave properties. The new model was applied to the three-dimensional LSTF experiments and accurately reproduced the measured wave runup. Inclusion of the slope-dependent surf-similarity parameter decreased the accuracy of the calculated wave runup as compared with the measured values.

An exception to the direct relationship between breaking wave height and runup concerns the presence of dune or beach scarping. The steep scarp substantially limits the uprush of swash motion, resulting in a much reduced maximum level, as compared with the nonscarping cases. For monochromatic waves, the measured wave runup was much smaller than the breaking wave height. The lack of low-frequency modulation limits the wave runup for monochromatic waves.

Based on the SUPERTANK and LSTF experiments, the upper limit of beach-profile change was found to be approximately equal to the total vertical excursion of wave runup. Therefore, the breaking wave height can be used to provide a reliable estimate of the limit of wave runup which, in turn, can serve as an approximation of the landward limit of beach change: $U_L = R_{tw} = H_{bs}$. Physical situations that are exceptions to this direct relationship are beaches with beach or dune scarps. For the scarped cases, the upper limit of beach change was much higher than the total swash runup and was controlled by the elevation of the berm or dune.

LITERATURE CITED

Baldock, T.E. and Holmes, P., 1999. Simulation and prediction of swash oscillation on a steep beach. *Coastal Engineering,* 36, 219–242.

Battjes, J.A., 1974. Computations of set-up, longshore currents, run-up overtopping due to wind-generated waves. *Report, 74-2.* Delft, the Netherlands: Delft University of Technology.

Bowen, A.J.; Inman, D.L., and Simmons, V.P., 1968. Wave "set-down" and "set-up." *Journal of Geophysical Research,* 73(8), 2569–2577.

Bruun, P., 1954. Coastal erosion and the development of beach profiles. *Technical Memo., No. 44.* Vicksburg, Mississippi: Beach Erosion Board, U.S. Army Corps of Engineers Waterways Experiment Station.

Coco, G., O'Hare, T.J., and Huntley, D.A., 1999. Beach cusps: a comparison of data and theories for their formation. *Journal of Coastal Research,* 15(3), 741–749.

Dean, R.G., 1977. Equilibrium beach profiles: U.S. Atlantic and Gulf coasts. *Ocean Engineering Report,* No. 12. Newark, Delaware: Department of Civil Engineering, University of Delaware.

Douglass, S.L., 1992. Estimating extreme values of run-up on beaches. *Journal of Waterway, Port, Coastal and Ocean Engineering,* 118, 220–224.

Guza, R.T. and Thornton, E.B., 1981. Wave set-up on a natural beach. *Journal of Geophysical Research,* 86(C5), 4133–4137.

Guza, R.T. and Thornton, E.B., 1982. Swash oscillations on a natural beach. *Journal of Geophysical Research,* 87(C1), 483–490.

Hamilton, D.G.; Ebersole, B.A.; Smith, E.R., and Wang, P., 2001. Development of a large-scale laboratory facility for sediment transport research. *Technical Report,* ERDC/SCH-TR-01-22. Vicksburg, Mississippi: U.S. Army Engineer Research and Development Center.

Hanslow, D. and Nielsen, P., 1993. Shoreline set-up on natural beaches. *Journal of Coastal Research,* Special Issue No. 15, pp. 1–10.

Hedges, T.S., and Mase, H., 2004. Modified Hunt equation incorporating wave setup. *Journal of Waterway, Port, Coastal and Ocean Engineering,* 130, 109–113.

Holland, K.T.; Raubenheimer, B.; Guza, R.T., and Holman, R.A., 1995. Runup kinematics on a natural beach. *Journal of Geophysical Research,* 100(C3), 4985–4993.

Holman, R.A., 1986. Extreme value statistics for wave run-up on a natural beach. *Coastal Engineering,* 9, 527–544.

Holman, R.A. and Sallenger, A.H., 1985. Setup and swash on a natural beach. *Journal of Geophysical Research,* 90(C1), 945–953.

Hunt, I.A., Jr., 1959. Design of seawalls and breakwaters. *Journal of the Waterways and Harbors Division,* 83(3), 123–152.

Huntley, D.A.; Davidson, M.; Russell, P.; Foote, Y., and Hardisty, J., 1993. Long waves and sediment movement on beaches: recent observations and implications for modeling. *Journal of Coastal Research,* 15, 215–229.

Kaminsky, G. and Kraus, N.C., 1994. Evaluation of depth-limited breaking wave criteria. *Proceedings of Ocean Wave Measurement and Analysis, Waves '94,* New York: ASCE Press, pp. 180–193.

Komar, P.D., 1998. *Beach Processes and Sedimentation.* Upper Saddle River, New Jersey: Prentice Hall, 544p.

Kraus, N.C. and Smith, J.M. (eds.), 1994. SUPERTANK Laboratory Data Collection project, Volume 1: Main text. *Technical Report CERC-94-3.* Vicksburg, Mississippi: U.S. Army Engineering Waterways Experiment Station, Coastal Engineering Research Center.

Kraus, N.C.; Smith, J.M., and Sollitt, C.K., 1992. SUPERTANK Laboratory data collection project. *In*: *Proceedings of the 23rd Coastal Engineering Conference,* ASCE, Venice, pp. 2191–2204.

Kriebel, D.L.; Kraus, N.C., and Larson, M., 1991. Engineering methods for predicting beach profile response. *In*: *Proceedings of the Coastal Sediments 1991,* ASCE, Seattle, pp. 557–571.

Larson, M.; Kubota, S., and Erikson, L., 2004. Swash-zone sediment transport and foreshore evolution: field experiments and mathematical modeling. *Marine Geology,* 212(1–4), 61–79.

Longuet-Higgins, M.S. and Stewart, R.W., 1962. Radiation stress and mass transport in gravity waves, with application to "Surf Beat." *Journal of Fluid Mechanics,* 13, 481–504.

Mase, H., 1988. Spectral characteristics of random wave run-up. *Coastal Engineering,* 12, 175–189.

Nielsen, P., 1988. Wave setup: a field study. *Journal of Geophysical Research,* 93(C12), 15, 643–652.

Nielsen, P. and Hanslow, D.J., 1991. Wave runup distributions on natural beaches. *Journal of Coastal Research,* 7(4), 1139–1152.

Puleo, J.A. and Holland, K.T., 2001. Estimating swash zone friction coefficients on a sandy beach. *Coastal Engineering,* 43, 25–40.

Roberts, T.M.; Wang, P., and Kraus, N.C., 2007. Limits of beach and dune erosion in response to wave runup elucidated from SUPERTANK. *In*: *Proceedings of Coastal Sediments 2007,* ASCE, New Orleans, pp. 1961–1973.

Ruesslink, B.G.; Kleinhans, M.G., and van den Beukel, P.G.L., 1998. Observations of swash under highly dissipative conditions, *Journal of Geophysical Research,* 103, 3111–3118.

Ruggiero, P.; Holman, R.A., and Beach, R.A., 2004. Wave run-up on a high-energy dissipative beach. *Journal of Geophysical Research,* 109(C06025), 1–12.

Ruggiero, P.; Komar, P.D.; McDougal, W.G.; Marra, J.J., and Beach, R.A., 2001. Wave runup, extreme water levels and the erosion of properties backing beaches. *Journal of Coastal Research,* 17(2), 407–419.

Sallenger, A.H., 2000. Storm impact scale for barrier island. *Journal of Coastal Research,* 16, 890–895.

Shen, M.C. and Meyer, R.E., 1963. Climb of a bore on a beach 3: run-up. *Journal of Fluid Mechanics,* 16, 113–125.

Stockdon, H.F.; Holman, R.A.; Howd, P.A., and Sallenger, A.H., 2006. Empirical parameterization of setup, swash, and runup. *Coastal Engineering,* 53, 573–588.

Suhayda, J.N., 1974. Standing waves on beaches. *Journal of Geophysical Research,* 79(21), 3065–3071.

Sunamura, T., 1984. Quantitative prediction of beach-face slopes. *Geological Society of America Bulletin,* 95, 242–245.

Wang, P. and Davis, R.A., Jr., 1998. A beach profile model for a barred coast—case study from Sand Key, west-central Florida. *Journal of Coastal Research,* 14, 981–991.

Wang, P.; Ebersole, B.A.; Smith, E.R., and Johnson, B.D., 2002. Temporal and special variations of surf-zone currents and suspended-sediment concentration. *Coastal Engineering,* 46, 175–211.

Wang, P.; Kirby, J.H.; Haber, J.D.; Horwitz, M.H.; Knorr, P.O., and Krock, J.R., 2006. Morphological and sedimentological impacts of Hurricane Ivan and immediate post-storm beach recovery along the northwestern Florida barrier-island coasts, *Journal of Coastal Research,* 22(6), 1382–1402.

Wang, P. and Kraus, N.C., 2005. Beach profile equilibrium and patterns of wave decay and energy dissipation across the surf zone elucidated in a large-scale laboratory experiment. *Journal of Coastal Research,* 21, 522–534.

Wang, P.; Smith, E.R., and Ebersole, B.A., 2002. Large-scale laboratory measurements of longshore sediment transport under spilling and plunging breakers. *Journal of Coastal Research,* 18, 118–135.

Yamamoto, Y.; Tanimoto, K., and Harshinie, K.G., 1994. Run-up of irregular waves on gently sloping beach. *In*: *Proceedings of the 23rd Coastal Engineering Conference,* ASCE, Venice, pp. 689–703.

APPENDIX: NOTATION

The following symbols are used in this paper.

A	shape parameter relating to grain size and fall velocity
C	wave velocity
f	friction coefficient
g	gravitational acceleration
h	still-water depth
H	wave height
H_b	breaking wave height
H_{bl}	local breaking wave height
H_{bs}	significant breaking wave height
$H_{b,h}$	high-frequency component of wave height at the breaker line
$H_{b,l}$	low-frequency component of wave height at the breaker line
h_l	local water depth
H_0	significant deep-water wave height
$H_{sl,h}$	high-frequency component of wave height at the shoreline line
$H_{sl,l}$	low-frequency component of wave height at the shoreline line
L_L	lower limit of beach change
L_0	deep-water wavelength
n	spectral peakedness parameter
N	Dean number
R_s	significant wave runup
$R_{sr,max}$	elevation of maximum swash uprush
R_{tw}	total wave runup
R_2	2% exceedance of runup
T	wave period
t_{max}	time of maximum swash excursion
T_p	peak spectral wave period
U_L	upper limit of beach change
V_0	initial velocity
V_x	velocity of a water particle in the across shore
w	sediment fall velocity
x	cross-shore coordinate; horizontal distance from the shoreline
$\tan \beta$	beach slope

tan β_f	foreshore beach slope	$\bar{\eta}$	wave setup
γ	breaker index	$\bar{\eta}_M$	wave setup under monochromatic waves
Δx	length of a water particle	$\bar{\eta}_{sl}$	wave setup at the shoreline
Δy	width of a water particle	ξ	surf-similarity parameter
Δz	height of a water particle	ρ	water density